

Rational and Statistical Approaches in Enhancing the Yield of Ethylene Carbonate in Urea Transesterification with Ethylene Glycol over Metal Oxides

Dina Fakhrnasova,^{†,‡} Ricardo J. Chimentão,^{‡,§} Francisco Medina,[‡] and Atsushi Urakawa^{*,†}

[†]Institute of Chemical Research of Catalonia (ICIQ), Av. Països Catalans 16, 43007 Tarragona, Spain

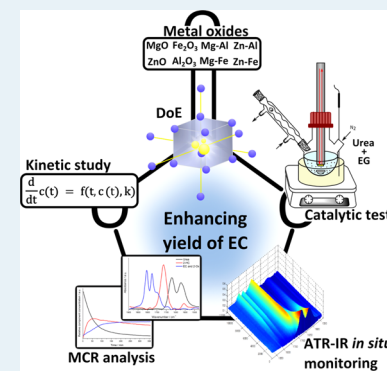
[‡]Departament d'Enginyeria Química, Universitat Rovira i Virgili, 43007 Tarragona, Spain

[§]School of Chemistry, Yachay Tech, Yachay City of Knowledge, 100119 Uruqui, Ecuador

Supporting Information

ABSTRACT: This work employs (i) a rational approach to improve the material properties of catalysts for urea transesterification with ethylene glycol (EG) to ethylene carbonate (EC) over metal oxides and (ii) a statistical approach to maximize the desired product. For the rational approach, single- and mixed-metal oxides with different elemental combinations (Zn, Mg, Al, Fe) with a variety of acid–base properties were synthesized and evaluated for the reaction. The roles of acidity and basicity in the identified reaction paths were clarified on the basis of product selectivities and kinetic parameters extracted from the concentration profiles of reactants and products in every reaction path by means of in situ IR monitoring and subsequent multivariate analysis. The paths toward EC are favorably catalyzed by acidic sites, while basic sites catalyze all paths toward undesired products. However, the surface sites are blocked when the acidity is too high and there exists an optimum value for the ratio of total acidic and basic sites to be an efficient catalyst in the targeted reaction. A mixed-metal oxide consisting of Zn and Fe at a 3:1 atomic ratio was found to be the optimum catalyst with a well-balanced acid–base property. Furthermore, a design of experiments (DoE) approach was used to statistically identify critical reaction parameters and optimize them for the best Zn- and Fe-containing catalysts. These approaches successfully gave insights into the determining material factors for the reaction and afforded excellent EC selectivity (up to 99.6%) with high yield.

KEYWORDS: mixed-metal oxides, transesterification, urea, ethylene glycol, ethylene carbonate, acid–base property, reaction mechanism, multivariate curve resolution, kinetics, DoE

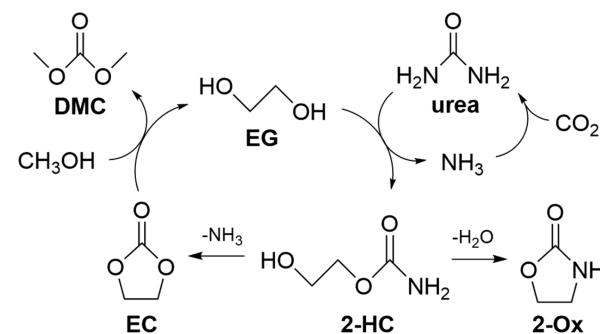


1. INTRODUCTION

Organic carbonates are a family of commercially important chemicals widely employed as intermediates¹ for a variety of synthetic and industrial applications and also as solvents.² Ethylene carbonate (EC) is a reactive starting and intermediate chemical³ for selective alkylation,⁴ carbamate formation,⁵ and transesterification⁶ to produce glycerol carbonate (GC)⁷ and linear carbonates such as dimethyl carbonate (DMC),⁸ which has drawn great attention as a green solvent, a phosgene replacement, and a fuel additive.⁹

DMC can be obtained in high yield via the transesterification reaction of EC with methanol. In this reaction, an equimolar amount of ethylene glycol (EG) is produced along with DMC (Scheme 1). This feature could be disadvantageous because of the different market demands for these two products. One approach to balance the amount of the two products at a desired ratio is to convert EG back to EC via transesterification of EG with urea, where NH₃ is coproduced. The EC synthesis in this route is advantageous for its mild operating pressure, low toxicity, and ease of handling of starting chemicals in addition to its high EC yield and selectivity, in comparison to the commercialized path of EC production by cycloaddition of

Scheme 1. Urea Transesterification with EG To Produce EC and To Close the Cycle of DMC Synthesis



CO₂ with ethylene oxide.¹⁰ In addition, the transesterification of EG with urea, synthesized from CO₂ and NH₃, can be considered as one path for indirect CO₂ utilization (Scheme 1).

Received: July 25, 2015

Revised: September 13, 2015

Published: September 15, 2015

This reaction has been reported to proceed in two steps (**Scheme 1**).¹¹ In the first step, urea reacts with EG to yield 2-hydroxyethyl carbamate (2-HC), and in the second step EC is formed by the elimination of NH₃ from 2-HC. The major challenge is to maximize the selectivity toward EC by avoiding side reactions such as the dehydration of 2-HC, forming the dominant side product, 2-oxazolidone (2-Ox).

Various solid catalysts have been investigated in the transesterification of EG with urea. Su and Speranza¹² described reactions of alkylene glycols and urea to synthesize alkylene carbonates using Sn-containing catalysts. More recently, a variety of metal oxides have been investigated in the reaction. Li¹³ has tested CaO, La₂O₃, MgO, ZnO, ZrO₂, and Al₂O₃ and found that ZnO is the most active and selective catalyst. An identical conclusion was drawn by Bhanager.¹⁴ Bhaduria¹⁵ studied Cr-containing zinc oxide materials, while Zhao³ investigated Fe-containing materials. In both studies the formation of the spinel phases (ZnCr₂O₄ and ZnFe₂O₄) was found to be important, promoting EC yield. The previous works agreed that a proper balance in the amount and nature of acidic and basic sites is important; however, their roles in each reaction step and in the overall reaction performance, i.e. yield of EC, have been unclarified.

To gain precise insights into the roles of acidic and basic sites in the reaction, we investigated the catalytic performance of single- and mixed-metal oxide materials consisting of Zn, Mg, Al, and/or Fe with distinct acid–base properties. Binary mixed-metal oxides were prepared via hydrotalcite precursors to achieve high surface area and homogeneous mixing of the resulting, typically nanosized metal oxide phases after calcination treatment. The reaction network influencing the yield of EC was identified, and every reaction path in the network was separately studied. The catalytic tests were performed with simultaneous monitoring of concentration evolutions of chemical species by means of a dip-in IR probe and multivariate analysis to extract kinetic information on every reaction path. The kinetic parameters, the yield of products, and acid–base properties of the materials determined by NH₃/CO₂-TPD, respectively, were holistically evaluated to elucidate the function of acid–base sites on the identified reaction paths, giving a comprehensive view of the strategies to rationally maximize EC yield. In addition, optimization of the reaction conditions was attempted with the best-performing catalyst by applying a contrasting method, namely a statistical method, the design of experiments (DoE). The results emphasize the usefulness of such mathematical approaches to maximize the selectivity and/or the yield of the target product influenced by each path in the complex reaction network.

2. EXPERIMENTAL SECTION

2.1. Catalysts and Materials. Mixed-metal oxides with the general formula M_b²⁺-M_t³⁺ containing Mg²⁺ or Zn²⁺ as a bivalent cation (M_b²⁺) and Al³⁺ or Fe³⁺ as a trivalent cation (M_t³⁺) with constant molar ratio M_b²⁺/M_t³⁺ = 3 were synthesized by a coprecipitation method. Mg²⁺-Al³⁺, Mg²⁺-Fe³⁺, and Zn²⁺-Al³⁺ mixed-metal oxides were synthesized as follows. An aqueous nitrate solution (100 mL) with an appropriate amount of the bivalent and trivalent cations was added dropwise into a beaker containing 100 mL of deionized water under vigorous stirring at room temperature. The pH of the solution was kept constant at 10 by adding a second aqueous solution of NaOH (2 M). The resultant slurry was aged for 18 h at room temperature, filtered, thoroughly washed

with deionized water, and dried at 373 K overnight. The resultant dried materials with the hydrotalcite structure were calcined at 723 K for 12 h to obtain the corresponding mixed-metal oxides. The synthesis of the single-metal oxides (ZnO, Al₂O₃, MgO, Fe₂O₃) followed the same protocol but used the aqueous solution of the respective nitrate precursor. Concerning the synthesis of the Zn²⁺-Fe³⁺ mixed-metal oxide, an aqueous solution of Na₂CO₃ (2 M) was used as the second solution because the resulting material after drying did not form a hydrotalcite structure when the NaOH solution was used. The precipitated solid was washed, dried, and calcined as described above. Hereafter, Mg²⁺-Al³⁺, Mg²⁺-Fe³⁺, Zn²⁺-Al³⁺, and Zn²⁺-Fe³⁺ mixed-metal oxides after calcination of the corresponding materials with hydrotalcite structures are denoted simply Mg-Al, Mg-Fe, Zn-Al, and Zn-Fe, respectively, or with “mixed oxide” after the simplified notation.

Sodium hydroxide (Alfa Aesar, 97%), zinc nitrate hexahydrate (Sigma-Aldrich, 98%), magnesium nitrate hexahydrate (Sigma-Aldrich, 98.0–102.0%), aluminum nitrate nonahydrate (Sigma-Aldrich, 98%), iron(III) nitrate nonahydrate (Alfa Aesar, 98.0–101.0%), sodium carbonate (Sigma-Aldrich, 99%), ethylene glycol (Alfa Aesar, 99%), urea (Alfa Aesar, 99–100.5%), 2-hydroxyethyl carbamate (Angene, 95%), ethylene carbonate (Sigma-Aldrich, 98%), and 2-oxazolidinone (Sigma-Aldrich, 98%) were used as received.

2.2. Catalyst Characterization. The surface area of the synthesized metal oxides was determined by N₂ physisorption (77 K) with the BET method using Autosorb 1-MP (Quantachrome) equipment. Acid–base properties of the materials were characterized by temperature-programmed desorption (TPD) of adsorbed CO₂ and NH₃, and the procedure was as follows. A sample (100 mg) was pretreated for 2 h at 723 K in He, cooled to 353 K, saturated with a gas containing the probe molecule (4.5% CO₂/5% NH₃ in He), and flushed afterward with He for 20 min. Subsequently, TPD measurements were performed at a heating rate of 20 K min⁻¹ under He flow (20 mL min⁻¹) and the quantity of desorbed gases was recorded by a TCD detector in TPDRO 1100 (Thermo Fisher Scientific). The amount of basic and acidic sites was calculated from the CO₂ and NH₃ peaks, respectively, after deconvolution of comprising desorption peaks using the PeakFit v4 software. It should be noted that single- and mixed-metal oxides are generally exposed to the reactive components of air after the synthesis and during the storage. For instance, Mg-containing materials readily adsorb and react with H₂O and CO₂ to form magnesium hydroxide and carbonate, affecting the acid–base properties of the materials.¹⁶ Therefore, it was important to treat the samples under a controlled atmosphere before the reaction and characterization (in our case high-temperature treatment at 723 K for 2 h in He) to remove the majority of the surface carbonates, as discussed later.

Powder X-ray diffraction (XRD) experiments were performed on a Bruker AXS D8 Advance diffractometer equipped with a Cu tube, a Ge (111) incident beam monochromator (λ 1.5406 Å), and a Vantec-1 PSD operated in transmission mode. Identification of the crystal phases was made by comparing with the reference data available in the Joint Committee on Powder Diffraction Standards (JCPDS).

2.3. Catalytic Test and in Situ IR Monitoring. Transesterification of urea with EG as well as reference reactions starting from the intermediates and products identified in the transesterification reaction were performed in a 25 mL three-necked flask equipped with a magnetic stirrer and a reflux

condenser. For the urea transesterification with EG, the reactor was initially charged with 89.51 mmol of EG and heated to a reaction temperature of 413 K. Subsequently, 8.33 mmol of urea and 0.16 g of catalyst (equivalent to 3 wt % of EG) were added to the solution and this point was considered as the starting point of the reaction. Catalyst material was pretreated at 723 K for 2 h under an He flow prior to the catalytic testing, and it was readily taken to the reactor to minimize exposure to the air. All reactions were performed for 6 h under an N₂ flow (0.5 L min⁻¹) to remove formed gaseous ammonia, which negatively affects the reaction performance. After 6 h of the reaction, the reactor was cooled to room temperature, the solid catalyst was separated from the solution by filtration, and the products in the solution were analyzed by GC (Agilent 6890N) equipped with an FID detector and an HP-35 capillary column and GC-MS (Agilent 6890N (GC) 5973 (MSD)) equipped with an HP-5 capillary column. In the case of the reactions starting from intermediates and products, 4.28 mmol of 2-HC, 5.11 mmol of EC, or 5.17 mmol of 2-Ox was charged into the reactor instead of urea, and the reactions were performed under identical conditions.

Product selectivity was calculated without taking into account the amount of 2-HC because other products are derived from 2-HC and neglecting 2-HC selectivity helps understand the preferred paths of the reactions. For the reaction of urea transesterification with EG as well as the reaction of 2-HC in EG, product selectivity was determined by the formula

$$S_{\text{product}} = [\text{product}] / ([\text{EC}] + [\text{2-Ox}] + [\text{DEG}] + [\text{TEA}] + [3-(2-\text{EtOH})-\text{2-Ox}]) \times 100$$

In case of the reaction of 2-Ox with EG

$$S_{\text{product}} = [\text{product}] / ([\text{2-Ox}] + [\text{TEA}] + [3-(2-\text{EtOH})-\text{2-Ox}]) \times 100$$

was used to obtain product selectivity. The yield of EC was expressed by the molar amount of EC produced per gram of catalyst due to inaccurate quantification of EG and urea caused by the excess of EG used and possible decomposition of urea into NH₃ and CO₂ during the reaction.

In all of the reactions examined in this work, the reaction mixture was also monitored with an in situ dip-in attenuated total reflection infrared (ATR-IR) spectroscopic probe (Mettler Toledo React-IR 4000 equipped with a diamond ATR crystal) by immersing the probe into the reaction solution. Spectra were recorded every 120 s at 4 cm⁻¹ resolution.

Furthermore, a multivariate analysis method, multivariate curve resolution (MCR),¹⁷ was employed for the analysis of the time-resolved IR data. MCR is a very powerful blind source and spectral separation method and allows disentangling overlapping spectral features on the basis of the kinetic resolution of comprising underlying spectral bands. The results of MCR analysis are the kinetically pure component spectra and their concentration profiles. This way of spectral analysis is significantly more precise in evaluating concentration profiles and kinetics in comparison to taking such information from the absorption band maxima because the latter method suffers from the overlaps of bands, which is common in IR spectroscopy and often leads to inaccurate extraction of kinetic parameters and incorrect data interpretations. The detailed procedure of the MCR and kinetic analysis used in this work is described in the Supporting Information.

3. RESULTS AND DISCUSSION

3.1. Catalyst Characterization.

3.1.1. XRD. The ordered layer structure characteristic of hydrotalcite was confirmed for all precursors of the mixed-metal oxides (Mg-Al, Mg-Fe, Zn-Al, Zn-Fe) examined in this work (XRD patterns are presented in Figure S1 in the Supporting Information). After calcination at 723 K in air, the hydrotalcite structure was destroyed and new metal oxide phases were formed (Figure S2 in the Supporting Information). The calcined materials showed the presence of oxides of bivalent cations (Zn²⁺ and Mg²⁺) as the major crystalline phase (hexagonal wurtzite or cubic periclase structure, respectively; Table 1) due to a ratio of 3 for M_b²⁺/

Table 1. BET Surface Area, Amount of Acidic and Basic Sites, and Identified Crystalline Phases of the Single- and Mixed-Metal Oxides

catalyst	BET surface area/m ² g ⁻¹	CO ₂ uptake/μmol g ⁻¹	NH ₃ uptake/μmol g ⁻¹	crystalline phase
Al ₂ O ₃	294	2.88	0.61	γ-Al ₂ O ₃
ZnO	4	0.31	0.01	wurtzite
MgO	165	6.27	0.02	periclase
Fe ₂ O ₃	25	1.00	0.01	hematite
Zn-Al	36	1.40	0.07	ZnO (wurtzite)
Zn-Fe	21	0.44	0.06	ZnO (wurtzite), ZnFe ₂ O ₄
Mg-Al	173	6.22	0.22	MgO (periclase)
Mg-Fe	113	3.22	0.15	MgO (periclase)

M_t³⁺ in the hydrotalcite structure. The Zn–Fe mixed oxide exhibits an additional phase of zinc franklinite (ZnFe₂O₄) as reported by Zhao et al.³ They observed the phase for Zn–Fe mixed oxides prepared by mechanical mixing of the corresponding metal precursors prior to a calcination treatment.

3.1.2. Textural Property. Specific surface areas of the metal oxides are presented in Table 1. The order of the values was Al₂O₃ > MgO > Fe₂O₃ > ZnO for the single-metal oxides. For the mixed-metal oxides, the major contributions made by the bivalent ions Zn²⁺ and Mg²⁺ to the surface areas were obvious. The trends in lowering or enhancing surface area given by the trivalent ions Al³⁺ and Fe³⁺ were also clearly visible and consistent with those observed for the corresponding single-metal oxides.

3.1.3. CO₂- and NH₃-TPD. The strength and the total amount of basic and acidic sites of the single- and mixed-metal oxides were characterized by TPD of CO₂ and NH₃, respectively. The amount of desorbed gases, corresponding to the amount of basic and acidic sites, is reflected in the peak area, whereas the desorption peak temperature indicates the strength of acidic and basic sites. Figure 1 presents the desorption profiles of CO₂ and NH₃ from the thermally treated catalysts (in He at 723 K). The quantified results are summarized in Table 1. TPD was performed up to 723 K, which is the same temperature as that used in the pretreatment before catalytic testing in order to characterize the relevant acidity and basicity of the catalysts in the reaction.

All metal oxides showed CO₂ desorption peaks with maxima at ca. 453 K. The Mg-containing materials MgO, Mg-Al, and Mg-Fe, exhibited a broad CO₂ desorption peak over a wide temperature range of 373–673 K with a maximum at 473 K, indicating the presence of a large number of basic sites with different strengths (weak, moderate and strong sites).¹⁸ Zn–Al,

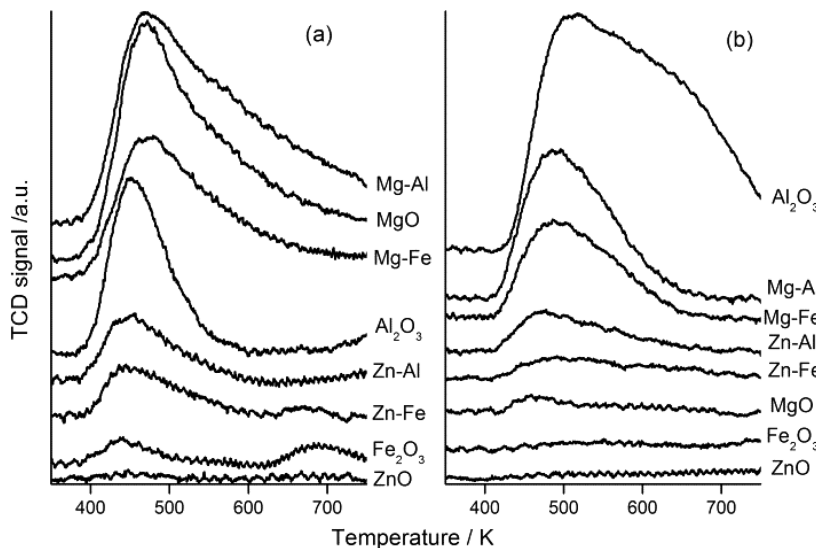


Figure 1. (a) CO_2 -TPD and (b) NH_3 -TPD profiles of the metal oxides.

Table 2. Product Selectivity in Urea Transesterification with Ethylene Glycol^a

catalyst	$Y_{\text{EC}}/(\text{mmol g}_{\text{cat}}^{-1})$	$S_{\text{EC}}/\%$	$S_{2\text{-Ox}}/\%$	$S_{\text{DEG}}/\%$	$S_{3\text{-(2-EtOH)-2-Ox}}/\%$	$S_{\text{TEA}}/\%$
blank	8.6	86.5	9.5	2.6	1.5	0
Al_2O_3	8.6	96.4	2.9	0	0	0
ZnO	18.4	73.7	15.9	5.1	3.5	1.8
MgO	19.4	83.2	8.3	4.1	3.0	1.5
Fe_2O_3	8.3	88.1	4.6	7.3	0	0
Zn-Al	20.1	82.0	9.7	4.0	2.8	1.6
Zn-Fe	25.9	91.5	5.1	3.5	0	0
Mg-Al	1.5	12.1	48.8	21.8	9.1	8.2
Mg-Fe	11.1	64.9	15.3	13.3	4.3	2.3

^aOnly products formed after 2-HC in the reaction paths have been considered (see Scheme 2; thus, the amount of 2-HC was not taken into account in the selectivity calculation). Reactions were performed at 413 K for 6 h starting with 89.51 mmol of EG, 8.33 mmol of urea, and 0.16 g of catalyst or without catalyst (blank) under N_2 flow (0.5 L min^{-1}).

ZnO , and Al_2O_3 showed narrower desorption peaks, compared to the Mg-containing materials, with the maxima at slightly lower temperatures of ca. 443 K. The differences indicate weaker and less types of available surface basic sites for Zn-Al , ZnO , and Al_2O_3 . In contrast, CO_2 desorption profiles of Zn-Fe and more notably of Fe_2O_3 showed an additional peak at a higher temperature of ca. 683 K, implying the presence of relatively strong surface basic sites in addition to the weaker sites for these two Fe-containing materials.

An NH_3 -TPD study of these materials clearly showed that Al_2O_3 , with the largest and broadest peaks of all samples examined, has highly acidic character with different (weak and strong) types of acidic sites. In contrast, other single-metal oxides (MgO , ZnO , and Fe_2O_3) showed very small or negligible NH_3 desorption peaks, indicating poor availability of surface acidic sites. However, it is interesting to observe that when Al^{3+} or Fe^{3+} cations are introduced to ZnO (i.e., Zn-Al , Zn-Fe), the acidity and basicity became more prominent, as confirmed by a larger peak of NH_3 and CO_2 desorption (Figure 1 and Table 1). Similar enhanced acidity and basicity by incorporation of foreign metal ions into the metal oxide structure have been reported.¹⁹ Also, the total amount of acidic sites of MgO was improved by incorporation of Al^{3+} and Fe^{3+} cations (i.e., Mg-Al , Mg-Fe). These results show that introducing metal cation(s) to a single metal oxide can enhance surface acid–base properties.

3.2. Urea Transesterification with EG. The chemical components of the reaction mixture were identified by means of GC-MS and quantified by GC analysis. Table 2 gives the product selectivity in the absence of a catalyst (blank) and in the presence of the metal oxides. In addition to the major reaction paths and products generally reported^{3,13,14} and described in Scheme 1, there were three other products identified. The first one was diethylene glycol (DEG), formed via the secondary ring-opening reaction of EC with EG accompanying a release of CO_2 (box B in Scheme 2). The other two products found in this work were 3-(2-hydroxyethyl)-2-oxazolidinone (3-(2-EtOH)-2-Ox) and triethanolamine (TEA) via the reaction of 2-Ox with EG (box C in Scheme 2). Bhanage¹⁴ reported secondary product formation possibly from reactions of EC and 2-Ox with EG, yielding 1-(2-hydroxyethyl)-2-imidazolidone and 3-(2-EtOH)-2-Ox. In addition, in a rare case a minor amount of ethylene urea (2-imidazolidone) was also found.¹⁴ In this work, 1-(2-hydroxyethyl)-2-imidazolidone and ethylene urea were not detected, and instead, DEG and TEA were identified for the first time to the best of our knowledge. As shown later, the reaction paths toward DEG from EC (box B) and 3-(2-EtOH)-2-Ox and TEA from 2-Ox (box C) shown in Scheme 2 were verified by testing the reactions starting from EC and 2-Ox with EG, respectively.

Scheme 2. Urea Transesterification with Ethylene Glycol: Identified Reaction Pathways

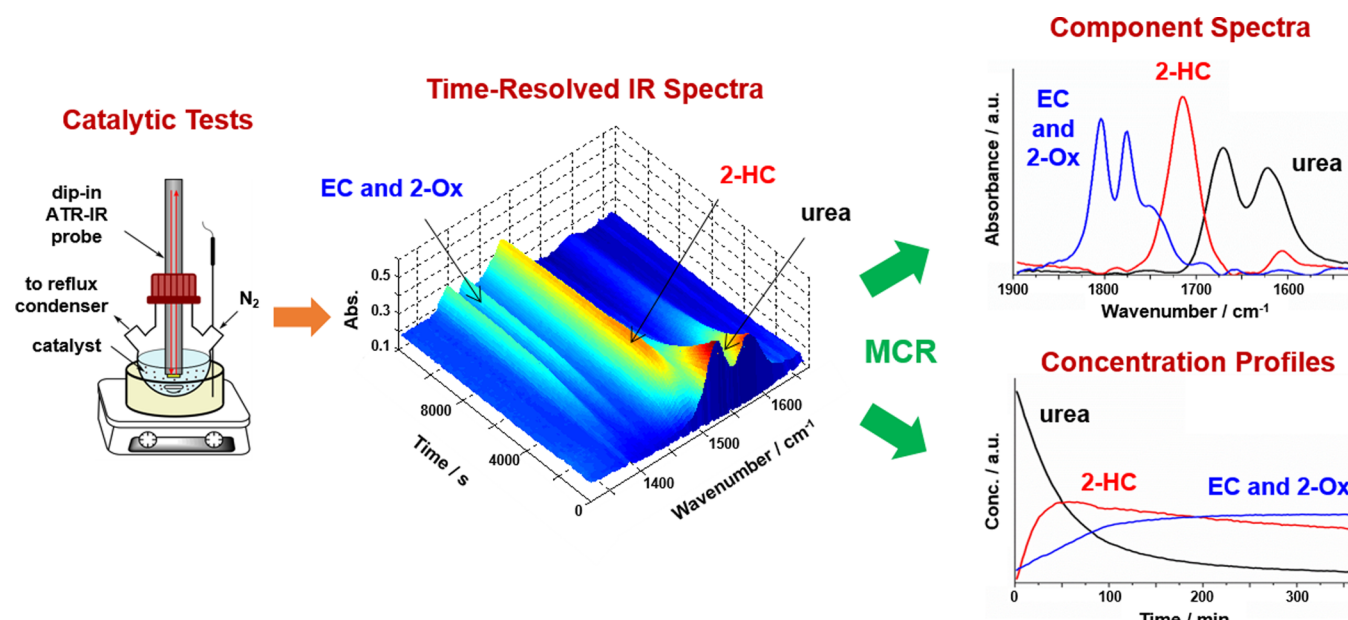
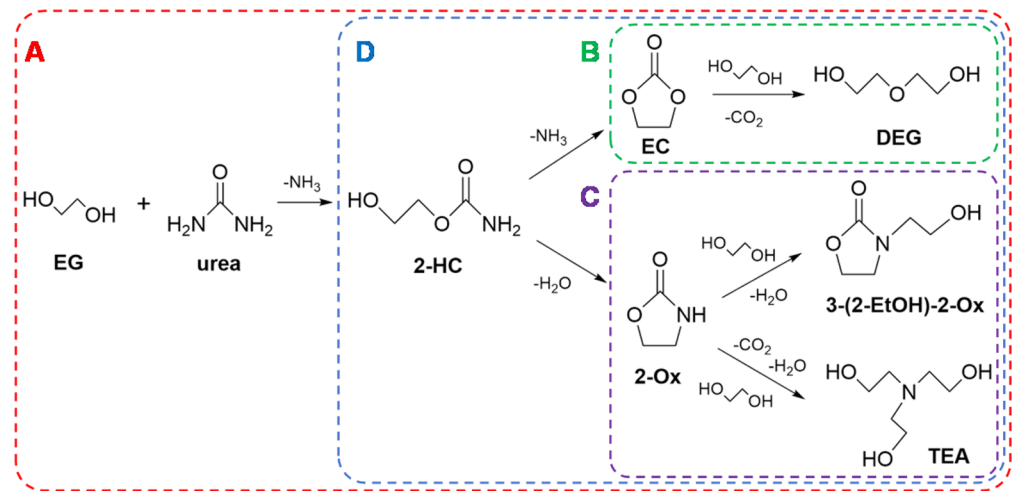


Figure 2. In situ IR monitoring of urea transesterification with EG and subsequent MCR analysis.

It is important to note that the reaction could proceed without catalyst to a moderate extent with a relatively high EC selectivity of 86.5% with 8.6 mmol g_{cat}⁻¹ EC yield and low but considerable (ca. 10%) selectivity to 2-Ox in addition to minor formation of DEG and 3-(2-EtOH)-2-Ox under the reaction conditions of this work after 6 h (Table 2). In contrast, Li¹³ reported that without catalyst no 2-Ox was found and the EC yield was relatively low after 3 h of the reaction at 423 K under vacuum (11 kPa) starting from 0.75 mol of EG and 0.5 mol of urea with 0.9 g of catalyst.

The type of metals in the catalyst and how the metal ions are combined in the mixed-metal oxides drastically affected both EC yield and product selectivity (Table 2). Regarding EC selectivity, most materials showed relatively high values except for Mg-containing mixed-metal oxides (Mg-Al and Mg-Fe). For these oxides, the selectivity to all undesired side products was very high, reaching even 48.8% 2-Ox for Mg-Al. In contrast, MgO showed high EC selectivity (83.2%). This indicates that Mg is not the sole factor to lower the EC selectivity. Al₂O₃ showed the highest EC selectivity (96.4%) of all materials

tested with a clearer product distribution: only 2-Ox as the single side product.

The best catalytic performance in terms of EC yield was obtained for Zn-Fe, showing 25.9 mmol g_{cat}⁻¹. The material effectively suppressed the formation of 2-Ox (5.1%) and the secondary reaction products, DEG, 3-(2-EtOH)-2-Ox, and TEA (the formation of the last two products was fully suppressed). The other Zn-containing mixed-metal oxide, Zn-Al, also showed high EC yield, but there was a noticeable increase in selectivity toward 2-Ox as well as secondary reaction products.

Furthermore, in situ IR monitoring of the reaction solution together with GC and MCR spectral analyses (Figure 2) was employed to investigate the reaction pathways and kinetics. The MCR analysis facilitated the extraction of comprehensive and quantitative concentration profiles of the major reactants, intermediates, and products during the course of the reaction for different catalyst materials. Performing the IR monitoring with the help of secondary reaction studies (testing the reaction from intermediate products) and product identification

confirmed that urea transesterification with EG to EC is a consecutive two-step process and also EC as well as 2-Ox can react further with EG (boxes B and C in **Scheme 2**)

To rationalize the factors influencing the reactivity and product selectivity at each reaction step, we divided and looked into the overall reaction with a wider and narrower scope of comprising reactions (**Scheme 2**): (A) overall reaction of urea transesterification, (B) EC decomposition with EG, (C) 2-Ox reaction with EG, and (D) 2-HC reaction in EG in the absence of urea. Reactions A–D were all monitored by the dip-in IR probe, and products were identified and quantified by GC. Thus, obtained concentration profiles of urea and products were used in the determination of reaction orders, reaction rate constants (k), and kinetic modeling of transesterification steps and overall process. The details of the kinetic modeling method and associated assumptions are described in the **Supporting Information**. Furthermore, the k values calculated for the single reaction steps were used for the rationalization of catalytic performance in relation to the amount of acidic and basic sites and also for a comparison with the k values estimated from the overall reaction, where the presence of other reactants and products may influence the kinetics of specific reaction paths.

In the overall reaction (box A), the urea conversion rate was found to apparently be second order (**Figure S3** and **Table S3** in the Supporting Information). We searched for the catalyst properties showing the best correlation to the reaction rate constant, and we identified that the total amount of acidic sites shows a clear trend with it (**Figure 3**). The reaction rate

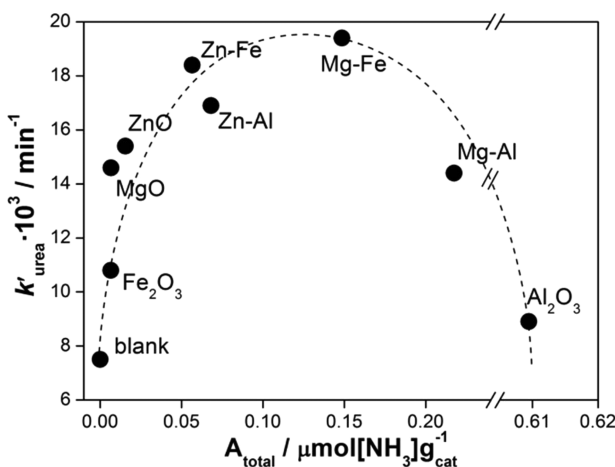


Figure 3. Urea reaction rate constant vs the total amount of acidic sites in urea transesterification with EG. The definition of k'_{urea} can be found in the **Supporting Information**. Dashed lines only serve to guide the eyes.

increases when the surface of the catalyst contains more acidic sites; however, if the catalyst surface possesses too many and/or too strong acidic sites, the urea reaction rate decreases, as observed for Mg-Al and Al₂O₃. Al₂O₃ showed the lowest urea reaction rate due to the high concentration of acidic sites and their overstrong character. Li et al.²⁰ concluded that the reaction between diols and urea was inhibited over acidic oxides to some extent, due to the formation of steady coordination of O and N atoms of urea to metal cations, which is in good agreement with our observations. Urea can be considered as a donor of electron pairs and a weakly basic molecule.²¹ As will be reported separately, urea interacts with and can adsorb strongly on the acidic sites of the catalyst (surface metal atoms

of metal oxides) via coordination of O atoms of the carbonyl group. Through such strong interactions of surface acidic sites and urea, surface catalytic sites might be poisoned for further reactions. This well explains the observed lower reaction rate of urea (**Figure 3**) when the catalyst contains more and stronger acidic sites.

3.3. Reaction of EC with EG. As described earlier, the desired target product (EC) reacts with EG, forming DEG accompanying a release of CO₂. This reaction takes place even in the absence of catalyst (**Table 2**) and should be avoided. Although the excess of EG present in the system as solvent makes prevention of this reaction path difficult, it is possible to fully suppress the formation of DEG as observed for Al₂O₃ (**Table 2**). In order to understand the nature of the reaction in light of the acidity and basicity of the catalysts, we have investigated the reaction path (box B, **Scheme 2**) by means of catalytic testing combined with *in situ* IR monitoring for all the catalysts.

The kinetic analysis of the EC concentration clarifies that EC conversion is apparently a first-order reaction and the rate constant was calculated assuming the reaction order (**Figure S5** and **Table S5** in the Supporting Information). Among the different possibilities, good correlation between EC conversion and its rate constant k and the amount of basic sites was found. **Figure 4** shows the plots of (a) EC conversion and (b) EC conversion rate constant against the total amount of basic sites determined by CO₂-TPD.

The EC conversion and its rate showed similar trends, as expected. Clearly, the reactivity of EC with EG increases when more basic sites are available on the catalyst surface. The materials with a small number of basic sites, e.g. Zn-containing materials, showed low activity in the reaction, whereas strongly basic Mg-containing materials exhibited high reactivity, even above 90% EC conversion to DEG using MgO. It is interesting to note that Fe₂O₃ showed high activity in the reaction, although it has a small amount of basic sites. The origin of the high activity might be attributed to the presence of strong basic sites, as demonstrated by CO₂-TPD analysis (**Figure 1a**). Also, Al₂O₃ showed small but some activity in the reaction, although DEG was not observed for the reaction starting from EG and urea as mentioned above. This may be attributed to the modification of acidity–basicity by the adsorption of urea and other products on the catalyst surface in urea transesterification with EG.

In the course of careful investigation on factors influencing EC conversion and DEG yield, we observed that catalyst pretreatment conditions can drastically affect the reactivity of the catalyst materials. Notably, DEG formation can be effectively suppressed by thermally treating catalysts under an inert atmosphere (He flow). **Figure 5** illustrates the DEG selectivity in the urea transesterification with EG over the metal oxides thermally treated at 723 K in He and also in air. Evidently, thermal treatment under an inert atmosphere led to the suppression of DEG formation. Carlson reported that the reaction between EC and alcohols (particularly glycols) or thioalcohols can be promoted in the presence of basic materials such as alkali carbonates.²² Therefore, it is probable that the thermal treatment in air permitted CO₂ in the atmosphere to react with the activated catalyst surface, forming surface carbonates with basic character which catalyzed the formation of DEG. Although the decomposition temperature of bulk inorganic carbonates is considerably higher (773–1173 K) than the pretreatment temperature used in this work (723 K),²³ the

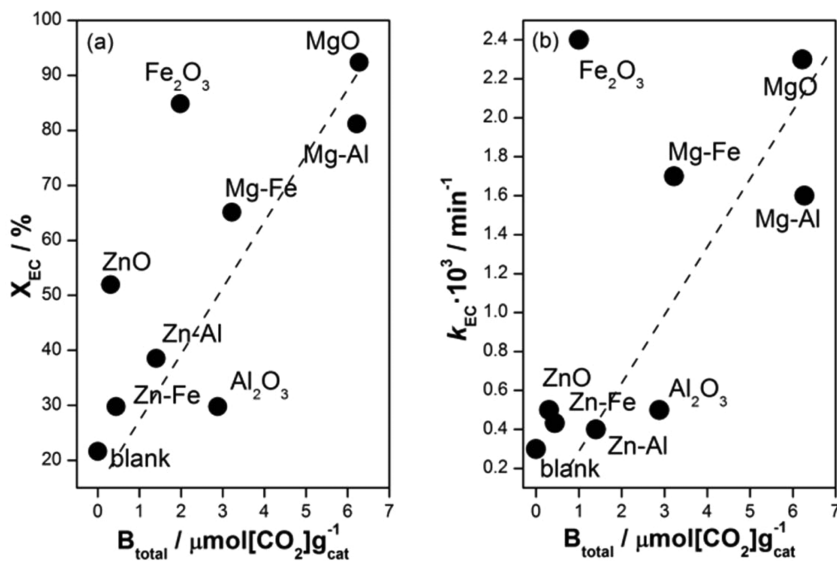


Figure 4. (a) EC conversion (X) and (b) EC reaction rate constant vs the total amount of basic sites. Reactions were performed for 6 h at 413 K. Dashed lines serve only to guide the eyes.

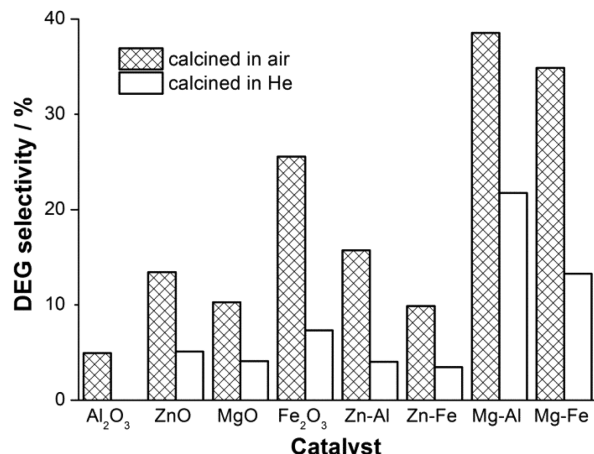


Figure 5. Selectivity to DEG in urea transesterification with EG for the catalysts calcined in the air and in He. Reactions were performed for 6 h at 413 K.

pretreatment is effective in keeping the surface less basic, most likely due to the lower decomposition/desorption temperature of CO_2 from the catalyst surface as observed in CO_2 -TPD (Figure 1a). Figure 5 clearly shows the importance of catalyst pretreatment under an inert atmosphere prior to catalytic testing. Therefore, we have employed the inert thermal treatment for all catalytic testing in this work.

3.4. Reaction of 2-Ox with EG. In a similar fashion, we have investigated one of the major undesired side reactions, i.e. reactions of 2-Ox with EG (Scheme 2, box C), producing TEA as the major product (ca. 90–95%) and also 3-(2-EtOH)-2-Ox as another byproduct (Table S2 in the Supporting Information). In situ IR monitoring clarified that the reactions between 2-Ox and EG apparently are a first order in 2-Ox concentration (Figure S6 and Table S6 in the Supporting Information).

Although the correlation between 2-Ox conversion or reaction rate and a specific characteristic of the catalysts was less obvious in comparison to the previous case of DEG

formation from EC and EG, there was a general trend observed between the reactivity and the amount of basic sites (Figure 6).

The relation of 2-Ox reactivity with the amount of basic sites was similar to that of EC reactivity (Figure 4), showing lower and higher 2-Ox reactivity for Zn- and Mg-containing materials, respectively. In addition, Fe_2O_3 promoted the reaction significantly as in the reaction between EC and EG likely due to the presence of strong basic sites (Figure 1a). It is worth noting that Zn-Fe with one of the lowest amount of basic sites (Table 1) converted only 14% of 2-Ox, whereas the reaction without catalyst (blank) results in 18% of 2-Ox conversion. On the basis of the higher initial reaction rate of 2-Ox using Zn-Fe in comparison to a few other materials (Figure 6b), the lowest 2-Ox conversion (Figure 6a) implies that the active sites of Zn-Fe were poisoned in the course of the reaction. This poisoning (more precisely selective site blocking) effect seems very effective starting from urea and EG, where no formation of TEA and 3-(2-EtOH)-2-Ox was observed using Zn-Fe (Table 2). Bhanage¹⁴ mentioned that catalysts with strong basic character such as CaO and La_2O_3 are highly active in the formation of 2-Ox and its further reaction products such as 3-(2-EtOH)-2-Ox, which is in accordance with the finding of this work. Hence, these undesired side reactions of 2-Ox are likely catalyzed by basic sites and are possibly prevented by reducing the number and/or weakening the strength of basic sites.

3.5. Reaction of 2-HC in EG. Furthermore, the reaction starting from the intermediate (2-HC) was investigated (Scheme 2, box D) to uncover the roles of acidic and basic sites toward the cyclization and the formation of EC or 2-Ox in the absence of urea in the reaction mixture. As observed in the overall reaction (Scheme 2A), EC and all other side products were detected with somewhat different product selectivity (Table S1 in the Supporting Information). In situ IR monitoring clarified that the EC and 2-Ox concentration rose at the expense of exponential decay in the 2-HC concentration and that the reaction is first order on 2-HC concentration (Figure S3 and Table S3 in the Supporting Information). With the aim of maximizing EC selectivity, factors such as the acidic and basic nature of catalysts influencing the cyclization selectivity to EC or 2-Ox were examined. After an extensive

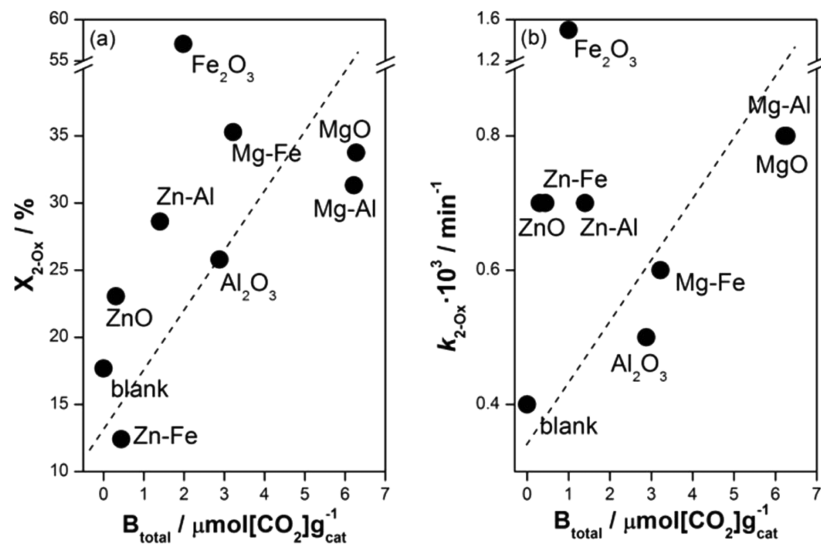


Figure 6. (a) 2-Ox conversion and (b) 2-Ox reaction rate constant vs the total amount of basic sites. Reactions were performed for 6 h at 413 K. Dashed lines serve only to guide the eyes.

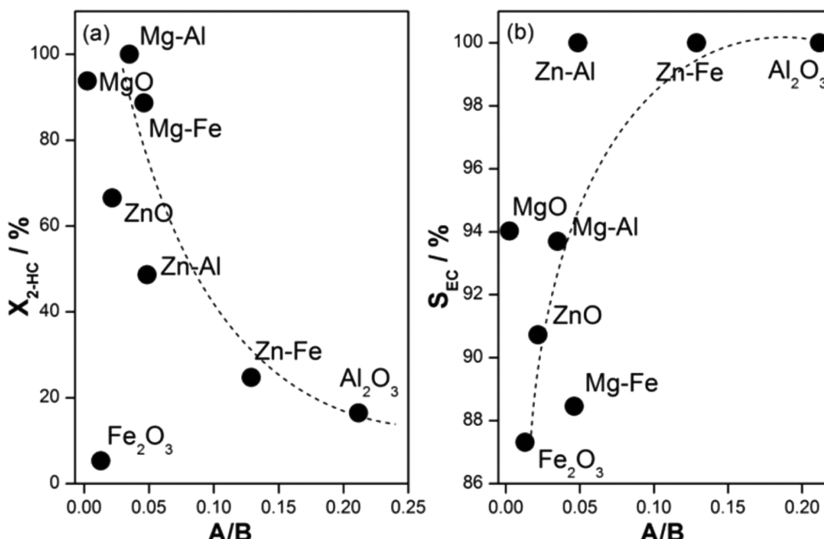


Figure 7. (a) 2-HC conversion and (b) EC selectivity vs the ratio between the total amount of acidic and basic sites (A/B). Reactions were performed for 6 h at 413 K. Dashed lines serve only to guide the eyes.

search, no obvious relation was found between 2-HC conversion or reaction rate and the number of acidic or basic sites (the total number of sites or site density calculated by scaling the total site number by the surface area of the materials). Hence, a more integral parameter representing the integrated acid–base properties of materials by taking the ratio between total amount of acidic and basic sites (A/B) was evaluated.

Figure 7 presents the plots of (a) 2-HC conversion and (b) EC selectivity (Table S1 in the Supporting Information) against A/B. A trend identical with 2-HC conversion was observed for the 2-HC reaction rate, and therefore, it is not shown for the sake of brevity. The metal oxides with a lower ratio of A/B, i.e. more basic material, exhibited very high conversion of 2-HC, reaching nearly full conversion as observed for Mg-containing materials (Figure 7a), with the exception of Fe_2O_3 showing low 2-HC conversion despite the low A/B value. In contrast, metal oxides with higher A/B values exhibit nearly full selectivity toward EC (Figure 7b). These materials, such as Al_2O_3 and Zn-

Fe, have a comparably higher amount of acidic sites and this property seems important to guide the reaction from 2-HC to the EC path (Scheme 2B) and not to 2-Ox path (Scheme 2C). Metal oxides with lower A/B values, i.e. more basic materials, showed deteriorated EC selectivity, guiding the reaction toward the 2-Ox path and also secondary reaction paths (Table S1). A high A/B value is important in guiding the reaction path toward EC formation as well as in suppressing the secondary reactions catalyzed by basic sites as previously clarified (3.3 and 3.4). When it comes to EC yield, the two factors—2-HC conversion as well as EC selectivity—directly contribute and the presence of well-balanced acidic and basic sites (A/B) is expected to be crucial.

3.6. Role of Acidic and Basic Sites in Urea Transesterification of EG. From the studies above, the variation of constituting elements in single-metal and mixed-metal oxides was found to drastically alter the acid–base properties of the materials and consequently influence reactivity, reaction paths, and EC yield. Fine tuning of acid–base properties and a

balanced proportion of surface acidic and basic sites are suggested to be critical for high EC yield with high selectivity on the basis of the reaction starting from 2-HC (Figure 7). The same conclusion is valid when the reaction starts from urea and EG (Scheme 2A). Figure 8 shows the EC yield in urea

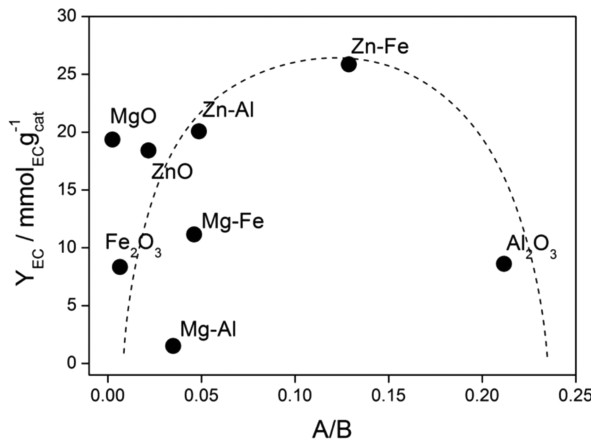


Figure 8. EC yield vs A/B ratio. Reactions were performed for 6 h at 413 K. Dashed lines serve only to guide the eyes.

transesterification with EG as a function of the A/B value. It shows the highest EC yield for a balanced A/B material (Zn-Fe), whereas lower EC yields were found for the more acidic or basic materials. The low basicity of Zn-Fe is important in driving the reaction more selectively toward EC, while the presence of weak acidity is important for urea activation without being poisoned (Figure 3).

The importance of balanced acid–base properties of catalyst materials in this or similar reactions has been concluded by other studies. Ball et al. reported that the reaction between primary and secondary alcohols with urea to form alkyl carbonates can be improved using an adequate combination of a weak Lewis acid and a Lewis base.¹¹ More recently, Climent et al.^{19a} concluded that the high activity and selectivity of Zn-Al mixed oxide in urea transesterification with glycerol can be attributed to well-balanced acid–base properties of the catalyst. Therein, cooperative effects between active sites created by different metal oxides were suggested; weakly Lewis-acidic metal sites activate the carbonyl group of the urea and Lewis basic sites activate glycerol. Wang et al.²⁴ investigated mixed Zn-Y oxides and demonstrated the importance of binary metal oxide phases, which resulted in catalytic activity higher than that of ZnO or Y₂O₃ due to the unique acid–base property given by the synergistic effects. Similar synergistic effects of Zn-Fe oxides were also reported by Zhao et al.³ They concluded that the formation of a ZnFe₂O₄ phase, as observed in our work, was responsible for the high catalytic performance. The presence of a unique phase where Zn and Fe are well mixed on an atomic scale in the oxide may be responsible for creating well-balanced acid–base sites in close vicinity and are thus favorable for the reaction.

Furthermore, we observed substantial differences in product selectivity when we start the reaction from urea and EG (Scheme 2A) or from 2-HC (Scheme 2D). The difference likely stems from the acid–base character of urea and also the modification of acidity and basicity upon its adsorption over the metal oxide surface. To gain detailed insights and highlight the influence of urea in the overall reaction paths, we compared the

reaction rate constants of the two reactions (i.e., starting from urea and EG or from 2-HC in EG). The reaction rate constants for 2-HC conversion in the urea + EG case were obtained from a fitting of the concentration profiles determined by in situ IR monitoring by varying rate constants. The details of the fitting procedure are described in the Supporting Information and the comparison of all rate constants is shown in Table S7 in the Supporting Information. The major difference lies in the rate constant for 2-HC conversion, which is given in Table 3.

Table 3. Reaction Rate Constants of 2-HC Conversion Starting from 2-HC in EG and from Urea and EG in the Presence and Absence of the Metal Oxides^a

catalyst	$k_{2\text{-HC}}/10^3 \text{ min}^{-1}$	
	2-HC and EG	urea and EG
blank	0.2	1.0
Al ₂ O ₃	0.4	1.1
ZnO	1.3	13.9
MgO	2.4	7.1
Fe ₂ O ₃	0.5	1.1
Zn-Al	0.8	8.2
Zn-Fe	0.6	10.4
Mg-Al	2.4	6.2
Mg-Fe	2.4	18.2

^aConfidence intervals of the rate constants (urea and EG) obtained by fitting are shown in Table S7 of the Supporting Information.

Clearly, the rate constants of 2-HC conversion starting from urea and EG are much higher than those starting from 2-HC in EG. For some catalysts such as ZnO and Mg-Fe, the 2-HC reaction rate boost was particularly prominent. According to the knowledge gained in this work (Figures 7 and 8), it is speculated that urea adsorbs on the acidic sites and renders the surface more basic, thus accelerating 2-HC conversion.

A higher 2-HC conversion rate is in principle advantageous to enhance EC yield, but this is only true when the path to EC is dominant in comparison to the path to 2-Ox (Scheme 2). To clarify the effects of urea on the selectivity from 2-HC toward EC or 2-Ox, we have compared the selectivity to the 2-Ox path as calculated by

$$\begin{aligned} \text{S(2-Ox path)} = & [2\text{-Ox}] + [\text{TEA}] + [2\text{-(1-EtOH)-2-Ox}] \\ & / ([\text{EC}] + [\text{DEG}] + [2\text{-Ox}] + [\text{TEA}] \\ & + [2\text{-(1-EtOH)-2-Ox}]) \times 100 \end{aligned}$$

Figure 9 shows the effect of the starting reaction conditions on the 2-Ox path selectivity. Generally, we observed remarkably higher selectivity toward the 2-Ox path when the reaction started from urea and EG. In other words, selectivity to EC can be drastically decreased in the presence of urea. These results suggest, as speculated earlier, that the poisoning by urea enhances the basic character of the surface, which drives the reaction toward the undesired 2-Ox path. The excellent catalyst Zn-Fe shows low 2-Ox path selectivity in the urea + EG reaction, with a value even lower than that of the blank reaction. This might be due to the fact that weakly acidic materials may not strongly adsorb urea and thus the enhancement of surface basicity is minimized, while in the liquid phase urea itself likely functions as a basic catalyst.

3.7. Catalyst Optimization. According to the studies above, we identified that a mixed oxide with a combination of

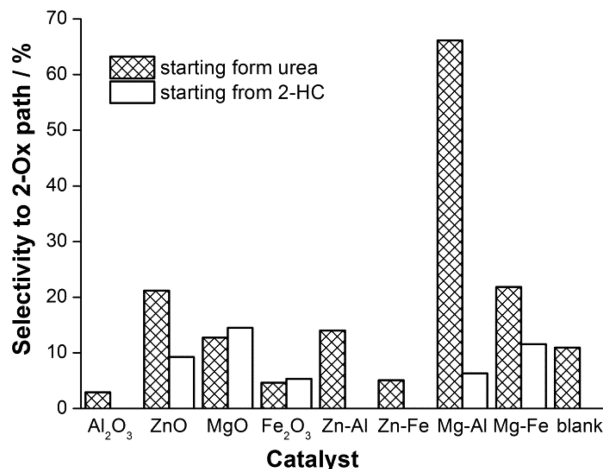


Figure 9. Selectivity to the 2-Ox path (Scheme 2C) against the EC path (Scheme 2B) starting from urea and EG (shadowed bar) or from 2-HC and EG (open bar). Reactions were performed for 6 h at 413 K.

Zn and Fe was particularly favorable for efficient EC synthesis by suppressing undesired side reactions due to its unique balance of acidity and basicity. Learning that A/B is an important parameter and that of Zn–Fe is optimal among the materials tested, we have attempted to synthesize Zn–Fe-based materials to cover A/B above and below the value of Zn–Fe (0.13, Figure 8). For this purpose, we have varied the Zn/Fe ratio (1/2, 6/1, and 9/1) or introduced a third metal (Mg or Al). In the former case, these oxides were produced by an identical method without formation of a hydrotalcite precursor. In the latter case molar ratio $\text{M}_b^{2+}/\text{M}_t^{3+} = 3$ was kept.

The syntheses were successful, as shown in Figure 10 (XRD patterns are shown in Figure S9 in the Supporting Information,

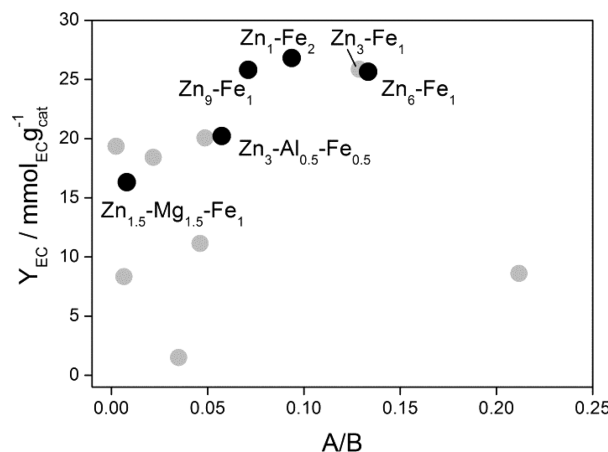


Figure 10. EC yield against A/B ratio of Zn–Fe-based oxides with different Zn/Fe molar ratios and the oxides with an additional third metal (Al or Mg). Gray markers are the data points taken from Figure 8. Reactions were performed for 6 h at 413 K.

and the material properties are summarized in Table S8 in the Supporting Information), mainly covering the lower A/B values except the material with Zn/Fe = 6/1 (denoted as Zn₆-Fe₁), which showed a slightly higher A/B value in comparison to that of Zn–Fe. In terms of EC yield, all of the materials synthesized followed the trends obtained previously. A slightly higher value of EC yield was obtained for the Zn–Fe material with a slightly lower A/B value (ca. 0.09; Zn₁-Fe₂) in comparison to that of

Zn–Fe. This A/B value represents the optimum A/B value to maximize EC yield. The addition of Mg or Al did not improve the acidity and basicity favorably, overenhancing the basic nature of the materials.

It is important to remark that the reaction performance in terms of product selectivity may not be satisfactory even when EC yields are high. Table S9 in the Supporting Information shows the EC yields and product selectivity of the additionally evaluated Zn–Fe-based materials. The best material in terms of EC yield (i.e., Zn₁-Fe₂) exhibited lower selectivity to EC and notably ca. 5% higher selectivity to DEG in comparison to Zn–Fe, which makes Zn–Fe a more attractive catalyst considering the slightly lower but comparable EC yield. The trimetallic oxides containing Mg or Al showed lower EC yield in comparison to the binary Zn–Fe family. Introduction of acidic Al resulted in an increase of EC selectivity, whereas introduction of Mg enhanced the basicity and consequently negatively affected the selectivity, as clearly visible from the high selectivity to DEG (42.6%). These effects are in full agreement with the previously suggested roles of acidic and basic sites.

This work has clarified that the acidity and basicity of catalyst materials play decisive roles in guiding the reaction path to specific and desired products. As a general observation, we remark that the reactions accompanying the release of NH₃ are catalyzed by acidic sites, whereas those accompanying the release of CO₂ and/or H₂O are catalyzed by basic sites. In Scheme 2, the first two important reactions toward EC, namely (i) urea + EG to 2-HC and (ii) 2-HC to EC are acid-catalyzed reactions, although overly strong acidic sites seem to be blocked by urea and therefore moderate acidity is important for urea activation and for better product yields. The other reactions, including the secondary reaction of EC to DEG and formation of 2-Ox and its secondary reactions, are identified to be catalyzed by basic sites. This simple and seemingly general trend would be very valuable to tune the catalyst acidity and basicity when reaction paths are identified from product distribution.

Among all materials investigated in this work, Zn–Fe (i.e., Zn₃-Fe₁) with a well-balanced acid–base property showed the best catalytic performance in terms of EC yield and selectivity. This material was selected for further reaction parameter optimization using a statistical approach presented in the following section.

3.8. Design of Experiments (DoE). We have uncovered the role of acidic and basic sites in the comprising reactions and their integrating effects on EC yield and selectivity in urea transesterification with EG. Apart from the important balance of acidic and basic sites, a large number of experimental parameters may influence the final outcome. To date, all studies have been devoted to finding the optimum reaction conditions for EC synthesis, where an examining-one-factor-at-a-time approach is used.^{3,14,24} Although this common approach can reveal how certain factors affect product yields, it explores the space of experimental parameters very poorly and also reveals little about the interaction (correlation) between these parameters for better optimization of the targeted quantity (here, EC yield and selectivity). With the aim of examining and demonstrating the power of statistical methods to efficiently identify experimental parameters affecting the targeted quantity and to optimize them with as few experiments as possible, we have employed a design of experiment (DoE)²⁵ method. The parameters considered as variables were reaction temperature,

reaction time, catalyst amount, and EG/urea ratio. The catalyst used was the best one we found in this work, Zn-Fe. We have used fractional factorial design in order to estimate the significance of the main effects and the interactions among various experimental parameters. Important variables were further optimized by central composite design. A detailed description of the DoE method is given in the *Supporting Information*.

The main factors influencing the selectivity of EC, 2-Ox, and DEG were found to be temperature and reaction time. This is reasonable due to the generally high effects of temperature on reactivity and product selectivity as well as to the fact that the reaction is of a consecutive nature; thus, an optimum reaction time is expected. Neither EG/urea ratio nor catalyst loading seemed to have considerable effects on the product distribution and EC yield, although the impacts of these parameters should be taken into account when process feasibility is evaluated. Additionally, interaction of the two parameters time and temperature with the parameters of interest (EC selectivity and yield) was found to be most significant. On the basis of identified important variables, models predicting EC selectivity (S_{EC}) and yield (Y_{EC}) in relation to reaction time and temperature were generated. The models for Y_{EC} and S_{EC} are displayed as response surfaces in Figures S11 and S12, respectively, in the Supporting Information.

According to the response surfaces, two optimum sets of reaction time and temperature were suggested to be advantageous to give high S_{EC} and Y_{EC} values: (1) 12 h at 399 K and (2) 2 h at 439 K. The reaction was performed under the two conditions with the standard conditions for the rest of the experimental parameters of this work using the Zn-Fe mixed oxide.

Both, very distinct, reaction conditions were highly beneficial for EC selectivity and yield. The first condition led to an excellent EC selectivity (99.6%) with a good EC yield (16 mmol g_{cat}⁻¹), while in the second case, a very high EC yield (28.59 mmol g_{cat}⁻¹) was obtained with a high EC selectivity (93.3%). In comparison to the previously achieved values for EC yield (25.9 mmol g_{cat}⁻¹) and selectivity (91.5%) at 423 K and 6 h, there is a clear advantage of DoE to improve the reaction parameters with a small number of tests, identifying importantly the reaction conditions we would not test otherwise. EC selectivity was maximized using the specific reaction conditions at a lower temperature, and the yield was maximized with the high reaction temperature but with the much shorter reaction time. This DoE study shows clearly the usefulness and effectiveness of statistical approaches to maximize the target product selectivity and yield in the complex, consecutive, and acid–base catalyzed reactions.

4. CONCLUSIONS

A series of single- and mixed-metal oxides, mostly derived from hydrotalcite precursors, consisting of four metal cations (Zn, Mg, Al, Fe) were synthesized with the aim of fine-tuning the acid–base properties. These materials were tested in urea transesterification with EG and in every comprising reaction pathway identified in this work. The concentration profiles of the reactants/products and kinetics parameters were obtained by means of IR monitoring using a dip-in ATR-IR probe with subsequent multivariate analysis (MCR). The roles of acidity and basicity at each reaction step have been unambiguously clarified from the relations between acidity and basicity of the

materials and the reaction performance or the kinetic information (reaction rate constants).

We could generalize that the reactions accompanying NH₃ release are acid-catalyzed and those accompanying CO₂ or H₂O release are base-catalyzed. The target product (EC) can be formed selectively over acidic sites; however, the surface reactivity is hindered when the acidity is too strong by urea adsorption (i.e., site blocking). The undesired product formation is catalyzed by basic sites. For these reasons, well-balanced amounts of acidic and basic sites are critical to achieve high EC yield with high EC selectivity. Among all of the materials tested, Zn-Fe material with 3/1 atomic ratio showed the best overall performance toward EC production.

Furthermore, a statistical approach (DoE) was used for the reaction where a number of experimental parameters influence the final quantity of interest in a very complex and dependent manner. This study demonstrated the usefulness and effectiveness of DoE in this reaction and suggested the same for complex acid–base catalyzed reactions in general. The DoE approach successfully identified experimental conditions where EC productivity and selectivity can be maximized with a small number of experiments for optimization. In summary, this study shows a holistic approach to improve the catalytic performance of a complex acid–base reaction on the basis of a combined rational (using structure–activity relationship) and statistical approach to efficiently maximize the yield of desired products.

■ ASSOCIATED CONTENT

● Supporting Information

The Supporting Information is available free of charge on the ACS Publications website at DOI: 10.1021/acscatal.5b01575.

XRD patterns of the metal oxides and precursors when they are derived from hydrotalcites, materials properties of Zn-Fe-based materials, and the procedures for MCR and kinetic analyses, fitting, and DoE (PDF)

■ AUTHOR INFORMATION

Corresponding Author

*E-mail for A.U.: aurakawa@iciq.es.

Notes

The authors declare no competing financial interest.

■ ACKNOWLEDGMENTS

D.F. and A.U. acknowledge financial support from the ICIQ Foundation and the MINECO (CTQ2012-34153) and also thank the MINECO for support through Severo Ochoa Excellence Accreditation 2014–2018 (SEV-2013-0319). R.J.C. acknowledges the Universitat Rovira i Virgili (URV) and Spanish Ministry of Science and Technology for financial support through the Juan de la Cierva program (JCI-2010-07328).

■ REFERENCES

- (1) Illuminati, G.; Romano, U.; Tesei, R. Process for the preparation of aromatic carbonates U.S. Patent 4,182,726, January 8, 1980.
- (2) Clements, J. H. *Ind. Eng. Chem. Res.* **2003**, *42*, 663–674.
- (3) Zhao, X.; An, H.; Wang, S.; Li, F.; Wang, Y. *J. Chem. Technol. Biotechnol.* **2008**, *83*, 750–755.
- (4) Clements, J. H.; Klein, H. P.; Marquis, E. T. Alkoxylation of 6-membered alkylene carbonates. U.S. Patent 6,498,278, December 24, 2002.

- (5) Webster, D. C.; Crain, A. L. Carbamate functional polymers and coatings thereof. U.S. Patent 2,002,006,514, January 17, 2002.
- (6) Buysch, H.-J.; Krimm, H.; Rüdolph, H. Process for the preparation of dialkyl carbonates. U.S. Patent 4,181,676, January 1, 1980.
- (7) Currier, V. A.; Bell, J. B.; Malkemus, J. D. Method for preparing glycerin carbonate. U.S. Patent 2,915,529, December 1, 1959.
- (8) Sharma, P.; Dwivedi, R.; Dixit, R.; Prasad, R. *Ind. Eng. Chem. Res.* **2013**, *52*, 10977–10987.
- (9) (a) Ono, Y. *Appl. Catal., A* **1997**, *155*, 133–166. (b) Pacheco, M. A.; Marshall, C. L. *Energy Fuels* **1997**, *11*, 2–29.
- (10) (a) Sachs, H. M. Preparation of alkylene carbonates. U.S. Patent 4,786,741, November 22, 1988. (b) Kao, J.-L.; Sheng, M. N. Preparation of alkylene carbonates from alkylene iodohydrins. U.S. Patent 4,231,937, November 4, 1980. (c) Raines, D. A.; Ainsworth, O. C. Ethylene carbonate process. U.S. Patent 4,233,221, November 11, 1980.
- (11) Ball, P.; Fullmann, H.; Heitz, W. *Angew. Chem., Int. Ed. Engl.* **1980**, *19*, 718–720.
- (12) Su, W.-Y.; Speranza, G. P. A process for preparing alkylene carbonates. US Patent 5,003,084, March 26, 1991.
- (13) Li, Q.; Zhang, W.; Zhao, N.; Wei, W.; Sun, Y. *Catal. Today* **2006**, *115*, 111–116.
- (14) Bhanage, B. M.; Fujita, S.; Ikushima, Y.; Arai, M. *Green Chem.* **2003**, *5*, 429–432.
- (15) Bhadauria, S.; Saxena, S.; Prasad, R.; Sharma, P.; Prasad, R.; R, D. *Eur. J. Chem.* **2012**, *3*, 235–240.
- (16) García-Sancho, C.; Moreno-Tost, R.; Mérida-Robles, J. M.; Santamaría-González, J.; Jiménez-López, A.; Maireles Torres, P. *Catal. Today* **2011**, *167*, 84–90.
- (17) Tauler, R. *Chemom. Intell. Lab. Syst.* **1995**, *30*, 133–146.
- (18) (a) Di Serio, M.; Ledda, M.; Cozzolino, M.; Minutillo, G.; Tesser, R.; Santacesaria, E. *Ind. Eng. Chem. Res.* **2006**, *45*, 3009–3014. (b) Menezes, A. O.; Silva, P. S.; Hernández, E. P.; Borges, L. E. P.; Fraga, M. A. *Langmuir* **2010**, *26*, 3382–3387.
- (19) (a) Climent, M. J.; Corma, A.; De Frutos, P.; Iborra, S.; Noy, M.; Velty, A.; Concepción, P. *J. Catal.* **2010**, *269*, 140–149. (b) Wang, H.; Yang, Y.; Xu, J.; Wang, H.; Ding, M.; Li, Y. *J. Mol. Catal. A: Chem.* **2010**, *326*, 29–40.
- (20) Li, Q.; Zhao, N.; Wei, W.; Sun, Y. *J. Mol. Catal. A: Chem.* **2007**, *270*, 44–49.
- (21) Newman, M. S.; Lala, L. K. *Tetrahedron Lett.* **1967**, *8*, 3267–3269.
- (22) Carlson, W. W. Process of hydroxyethylation. U.S. Patent 2,448,767, September 7, 1948.
- (23) Rowland, R. A. *Clays Clay Miner.* **1952**, *1*, 151–163.
- (24) Wang, P.; Liu, S.; Zhou, F.; Yang, B.; Alshammary, A. S.; Lu, L.; Deng, Y. *Fuel Process. Technol.* **2014**, *126*, 359–365.
- (25) Esbensen, K. H.; Guyot, D.; Westad, F.; Houmoller, L. P. *Multivariate Data Analysis - In Practice: An Introduction to Multivariate Data Analysis and Experimental Design; Multivariate Data Analysis*, 2002.